J|A|C|S ARTICLES

Published on Web 12/09/2010

Record Ferromagnetic Exchange through Cyanide and Elucidation of the Magnetic Phase Diagram for a $Cu^{II}Re^{IV}(CN)_2$ Chain Compound

T. David Harris,[†] Claude Coulon,[‡,§] Rodolphe Clérac,*[,‡,§] and Jeffrey R. Long*[,†]

Department of Chemistry, University of California, Berkeley, California 94720, United States, Université de Bordeaux, UPR 8641, Pessac F-33600, France, and CNRS, UPR 8641, Centre de Recherche Paul Pascal (CRPP), Equipe "Matériaux Moléculaires Magnétiques", 115 avenue du Dr. Albert Schweitzer, 33600 Pessac, France

Received September 30, 2010; E-mail: jrlong@berkeley.edu; clerac@crpp-bordeaux.cnrs.fr

Abstract: Reaction of the high-magnetic anisotropy building unit $[ReCl_4(CN)_2]^{2-}$ with $[Cu(MeCN)_6]^{2+}$ and hydrotris(pyrazol-1-yl)borate (Tp^-) affords the zigzag chain compound $(Bu_4N)[TpCuReCl_4(CN)_2]$. Dc magnetic susceptibility measurements reveal the presence of ferromagnetic exchange coupling between Re^{IV} and Cu^{II} centers along each chain and a fit to the data gives an exchange constant of $J/k_B = +41$ K ($+29$ cm^{-1}), representing the strongest ferromagnetic coupling yet observed through cyanide. Below 11.4 K and at applied fields of less than 3600 Oe, the compound undergoes a phase transition to an antiferromagnetic ground state, stemming from weak $\pi-\pi$ interchain interactions of strength $J_\perp/k_B = -1.7$ K (-1.2 cm^{-1}). This metamagnetic behavior is fully elucidated using both experimental and theoretical methods. In addition, theoretical modeling provides a detailed determination of the local anisotropy tensors corresponding to the $[ReCl_4(CN)_2]^{2-}$ units and demonstrates that the zigzag arrangement of the Re^{IV} centers significantly reduces the effective anisotropy of the chain. These results demonstrate the utility of the $Re^{IV}-CN-Cu^{II}$ linkage and the importance of anisotropic spin orientation in designing strongly coupled systems, which will aid in both the realization of single-chain magnets with higher relaxation barriers and in the construction of high-dimensional cyano-bridged materials exhibiting higher ordering temperatures.

Introduction

Cyano-bridged compounds have played an integral role in the development of coordination chemistry, beginning with the initial report of Prussian Blue over three centuries ago.[1] Through the years, scientists have learned to utilize the structural rigidity and predictability of the cyanide ligand to create a myriad of structure types, including multinuclear cyano-bridged clusters[2,3] and extended solids exhibiting one-, two-, and three-dimensional frameworks.[4] Perhaps more importantly, this structural diversity has given rise to compounds that display a wide range of physical properties that lend themselves to practical applications, such as molecular sieve technology, gas storage and separation, heterogeneous catalysis, and ion exchange.[4b,5] In addition, the ability of the cyanide ligand to mediate magnetic superexchange has led to a confluence of cyanide chemistry and molecule-based magnet research over the past two decades.[2−4] Indeed, these recent efforts have already resulted in low-density permanent magnets that order above room temperature,[4e,l,m] in addition to a number of single-molecule[6] and single-chain magnets[7] possessing high barriers to magnetic relaxation. Considering the field of cyano-bridged magnetic materials as a whole, one common theme emerges among the compounds: they would all benefit from stronger magnetic exchange interactions. Indeed, the strength through which paramagnetic centers are coupled is directly proportional to the magnetic ordering temperatures of bulk solids, the relaxation barriers of single-chain magnets, and the ground state isolation in single-molecule magnets.

Despite the importance of exchange strength in magnetic materials, the compounds displaying the strongest coupling

[†] University of California.
[‡] Université de Bordeaux.
[§] CNRS, Centre de Recherche Paul Pascal.

(1) (a) Anonymous, *Misc. Berlinensia Incrementum Scientarium (Berlin)* **1710**, *1*, 377. (b) Woodward, J. *Phil. Trans.* **1724**, *33*, 15. (c) Brown, J. *Phil. Trans.* **1724**, *33*, 19.

(2) (a) Long, J. R. Molecular Cluster Magnets. In *Chemistry of Nanostructured Materials*; Yang, P., Ed.; World Scientific: Hong Kong, 2003; pp 291−315, and references therein. (b) Beltran, L. M. C.; Long, J. R. *Acc. Chem. Res.* **2005**, *38*, 325. (c) Shatruk, M.; Avendano, C.; Dunbar, K. In *Progress in Inorganic Chemistry*; Karlin, K. D., Ed.; John Wiley & Sons: Amsterdam, 2009; Vol. 56, pp 155, and references therein.

(3) Selected references: (a) Mallah, T.; Auberger, C.; Verdaguer, M.; Veillet, P. *Chem. Commun.* **1995**, 61. (b) Parker, R. J.; Hockless, D. C. R.; Moubaraki, B.; Murray, K. S.; Spiccia, L. *Chem. Commun.* **1996**, 2789. (c) Zhong, Z. J.; Seino, H.; Mizobe, Y.; Hidai, M.; Fujishima, A.; Ohkoshi, S.-I.; Hashimoto, K. *J. Am. Chem. Soc.* **2000**, *122*, 2952. (d) Marvaud, V.; Decroix, C.; Scuiller, A.; Guyard-Duhayon, C.; Vaissermann, J.; Gonnet, F.; Verdaguer, M. *Chem.—Eur. J.* **2003**, *9*, 1677. (e) Li, D.; Parkin, S.; Wang, G.; Yee, G. T.; Prosvirin, A. V.; Holmes, S. M. *Inorg. Chem.* **2005**, *44*, 4903. (f) Ni, Z.-H.; Kou, H.-Z.; Zhang, L.-F.; Ge, C.; Cui, A.-L.; Wang, R.-J.; Li, Y.; Sato, O. *Angew. Chem., Int. Ed.* **2005**, *44*, 7742. (g) Harris, T. D.; Long, J. R. *Chem. Commun.* **2007**, 1360. (h) Shatruk, M.; Dragulescu Andrasi, A.; Chambers, K. E.; Stoian, S. A.; Bominaar, E. L.; Achim, C.; Dunbar, K. R. *J. Am. Chem. Soc.* **2007**, *129*, 6104. (i) Wang, X.-Y.; Prosvirin, A. V.; Dunbar, K. R. *Angew. Chem., Int. Ed.* **2010**, *122*, 5135.

through cyanide exhibit antiferromagnetic interactions.[4e,l,m,8] This coupling aligns spins on neighboring metal centers such that their moments oppose one another, thereby minimizing the overall moment and offsetting the positive effects of strong coupling. As such, the installation of stronger ferromagnetic interactions between metal centers presents a formidable challenge in designing new magnetic materials. One potential strategy to accomplish this goal is to construct a compound with $M-CN-Cu^{II}$ linkages, where M features a t_{2g}^3 electronic configuration. Here, the Cu^{II} ion bears a single unpaired electron, residing in a $d_{x^2-y^2}$ orbital, along the direction of exchange coupling through the cyanide ligand.[2c,3d,9] Moreover, the σ-type orbital in which the electron resides is orthogonal to the π-type orbitals of the other metal center, thus giving rise to ferromagnetic exchange. With this in mind, we have begun targeting compounds composed of Cu^{II} centers connected to $[ReCl_4(CN)_2]^{2-}$ units.

In addition to the requisite t_{2g}^3 configuration, $[ReCl_4(CN)_2]^{2-}$ has been shown to exhibit very strong uniaxial magnetic anisotropy and has consequently been employed to direct the formation of a series of single-chain magnets, $(DMF)_4MReCl_4(CN)_2$ (M = Mn, Fe, Co, Ni).[10] The slow magnetization dynamics in these solids occur despite weak intrachain coupling between the Re^{IV} and M^{II} centers, as the magnitude of this coupling, J, has been shown to partially govern the overall relaxation barrier ($\Delta_\tau = (8J + D)S^2$ in the Ising limit).[11] Thus, increasing the strength of this exchange should result in an increase in barrier height. Importantly, however, in strongly correlated one-dimensional systems even weak interactions between neighboring chains can result in the breakdown of low-dimensional magnetic behavior, giving rise instead to long-range magnetic ordering. As such, it is critical not only to increase the strength of magnetic interactions along each chain, but also to understand the role interchain interactions play in the overall magnetic behavior of the solid.

Herein, we report the formation of the cyano-bridged chain compound $(Bu_4N)[TpCuReCl_4(CN)_2]$, which displays the strongest ferromagnetic exchange yet observed through the cyanide ligand. In addition, weak $\pi-\pi$ interactions between neighboring chains are shown to induce a magnetic phase transition at 11.4 K to give an antiferromagnetic ground state. To understand the origins of this effect, a suite of dc magnetic measurements have been employed to provide a complete mapping of the metamagnetic behavior of the compound as a function of temperature and applied field. Moreover, this behavior, which is common to many magnetic chain compounds, is understood in micro-

(4) Selected references: (a) Shriver, D. F.; Shriver, S. A.; Anderson, S. E. *Inorg. Chem.* **1965**, *4*, 725. (b) Buser, H. J.; Schwarzenbach, D.; Petter, W.; Ludi, A. *Inorg. Chem.* **1977**, *16*, 2704. (c) Mallah, T.; Thiebaut, S.; Verdaguer, M.; Veillet, P. *Science* **1993**, *262*, 1554. (d) Gadet, V.; Mallah, T.; Castro, I.; Verdaguer, M.; Veillet, P. *J. Am. Chem. Soc.* **1992**, *114*, 9213. (e) Ferlay, S.; Mallah, T.; Ouahes, R.; Veillet, P.; Verdaguer, M. *Nature* **1995**, *378*, 701. (f) Entley, W. R.; Girolami, G. S. *Science* **1995**, *268*, 397. (g) Dunbar, K. R.; Heintz, R. A. *Prog. Inorg. Chem.* **1997**, *45*, 283, and references therein. (h) Larionova, J.; Clérac, R.; Sanchiz, J.; Kahn, O.; Golhen, S.; Ouahab, L. *J. Am. Chem. Soc.* **1998**, *120*, 13088. (i) Verdaguer, M.; Bleuzen, A.; Marvaud, V.; Vaissermann, J.; Seuleiman, M.; Desplanches, C.; Scuiller, A.; Train, C.; Garde, R.; Gelly, G.; Lomenech, C.; Rosenman, I.; Veillet, P.; Cartier, C.; Villain, F. *Coord. Chem. Rev.* **1999**, *190−192*, 1023, and references therein. (j) Larionova, J.; Kahn, O.; Golhen, S.; Ouahab, L.; Clérac, R. *Inorg. Chem.* **1999**, *38*, 3621. (k) Larionova, J.; Kahn, O.; Golhen, S.; Ouahab, L.; Clérac, R. *J. Am. Chem. Soc.* **1999**, *121*, 3349. (l) Holmes, S. M.; Girolami, G. S. *J. Am. Chem. Soc.* **1999**, *121*, 5593. (m) Hatlevik, O.; Buschmann, W. E.; Zhang, J.; Manson, J. L.; Miller, J. S. *Adv. Mater.* **1999**, *11*, 914. (n) Liao, Y.; Shum, W. W.; Miller, J. S. *J. Am. Chem. Soc.* **2002**, *134*, 9336. (o) Verdaguer, M.; Girolami, G. In *Magnetism: Molecules to Materials V*; Miller, J. S., Drillon, M., Eds.; Wiley-VCH: Weinheim, 2005; p 283. (p) Tomono, K.; Tsunobuchi, Y.; Nakabayashi, K.; Ohkoshi, S. *Inorg. Chem.* **2010**, *49*, 1298. (q) Her, J.-H.; Stephens, P. W.; Kareis, C. M.; Moore, J. G.; Min, K. S.; Park, J.-W.; Bali, G.; Kennon, B. S.; Miller, J. S. *Inorg. Chem.* **2010**, *49*, 1524.

(5) (a) Seifer, G. B. *Russ. J. Inorg. Chem.* **1959**, *4*, 841. (b) Loos-Neskovic, C.; Fedoroff, M.; Garnier, E. *Talanta* **1989**, *36*, 749. (c) Kuyper, J.; Boxhoorn, G. *J. Catal.* **1987**, *105*, 163. (d) Kaye, S. S.; Choi, H. J.; Long, J. R. *J. Am. Chem. Soc.* **2008**, *130*, 16921.

(6) Selected references: (a) Sokol, J. J.; Hee, A. G.; Long, J. R. *J. Am. Chem. Soc.* **2002**, *124*, 7656. (b) Berlinguette, C. P.; Vaughn, D.; Cañada-Vilalta, C.; Galán-Mascarós, J. R.; Dunbar, K. R. *Angew. Chem., Int. Ed.* **2003**, *42*, 1523. (c) Schelter, E. J.; Prosvirin, A. V.; Dunbar, K. R. *J. Am. Chem. Soc.* **2004**, *126*, 15004. (d) Song, Y.; Zhang, P.; Ren, X.-M.; Shen, X.-F.; Li, Y.-Z.; You, X.-Z. *J. Am. Chem. Soc.* **2005**, *127*, 3708. (e) Wang, C.-F.; Zuo, J.-L.; Bartlett, B. M.; Song, Y.; Long, J. R.; You, X.-Z. *J. Am. Chem. Soc.* **2006**, *128*, 7162. (f) Glaser, T.; Heidemeier, M.; Weyhermüller, T.; Hoffmann, R.-D.; Rupp, H.; Müller, P. *Angew. Chem., Int. Ed.* **2006**, *45*, 6033. (g) Lim, J. H.; Yoon, J. H.; Kim, H. C.; Hong, C. S. *Angew. Chem., Int. Ed.* **2006**, *45*, 7424. (h) Li, D.; Parkin, S.; Wang, G.; Yee, G. T.; Prosvirin, A. V.; Holmes, S. M. *Inorg. Chem.* **2005**, *44*, 4903. (i) Freedman, D. E.; Jenkins, D. M.; Iavarone, A. T.; Long, J. R. *J. Am. Chem. Soc.* **2008**, *130*, 2884. (j) Yoshihara, D.; Karasawa, S.; Koga, N. *J. Am. Chem. Soc.* **2008**, *130*, 10460. (k) Zadrozny, J. M.; Freedman, D. E.; Jenkins, D. M.; Harris, T. D.; Iavarone, A. T.; Harté, E.; Mathonière, C.; Clérac, R.; Long, J. R. *Inorg. Chem.* **2010**, *49*, 8886.

(7) (a) Lescouëzec, R.; Vaissermann, J.; Ruiz-Pérez, C.; Lloret, F.; Carrasco, R.; Julve, M.; Verdaguer, M.; Dromzée, Y.; Gatteschi, D.; Wernsdorfer, W. *Angew. Chem., Int. Ed.* **2003**, *42*, 1483. (b) Toma, L. M.; Lescouëzec, R.; Lloret, F.; Julve, M.; Vaissermann, J.; Verdaguer, M. *Chem. Commun.* **2003**, 1850. (c) Wang, S.; Zuo, J.-L.; Gao, S.; Song, Y.; Zhou, H.-C.; Zhang, Y.-Z.; You, X.-Z. *J. Am. Chem. Soc.* **2004**, *126*, 8900. (d) Toma, L. M.; Delgado, F. S.; Ruiz-Pérez, C.; Carrasco, R.; Cano, J.; Lloret, F.; Julve, M. *Dalton. Trans.* **2004**, 2836. (e) Ferbinteanu, M.; Miyasaka, H.; Wernsdorfer, W.; Nakata, K.; Sugiura, K.; Yamashita, M.; Coulon, C.; Clérac, R. *J. Am. Chem. Soc.* **2005**, *127*, 3090. (f) Wen, H.-R.; Wang, C. F.; Song, Y.; Gao, S.; Zuo, J.-L.; You, X.-Z. *Inorg. Chem.* **2006**, *45*, 8942. (g) Toma, L. M.; Lescouëzec, R.; Pasán, J.; Ruiz-Pérez, C.; Vaissermann, J.; Cano, J.; Carrasco, R.; Wernsdorfer, W.; Lloret, F.; Julve, M. *J. Am. Chem. Soc.* **2006**, *128*, 4842. (h) Costa, V.; Lescouëzec, R.; Vaissermann, J.; Herson, P.; Journaux, Y.; Araujo, M. H.; Clemente-Juan, J. M.; Lloret, F.; Julve, M. *Inorg. Chim. Acta* **2008**, *361*, 3912. (i) Choi, S. W.; Kwak, H. Y.; Yoon, J. H.; Kim, H. C.; Koh, E. K; Hong, C. S. *Inorg. Chem.* **2008**, *47*, 10214. (j) Visinescu, D.; Madalan, A. M.; Andruh, M.; Duhayon, C.; Sutter, J.-P.; Ungur, L.; Van den Heuvel, W.; Chibotaru, L. F. *Chem.−Eur. J.* **2009**, *15*, 11808. (k) Yoo, H. S.; Ko, H. H.; Ryu, D. W.; Lee, J. W.; Yoon, J. H.; Lee, W. R.; Kim, H. C.; Koh, E. K.; Hong, C. S. *Inorg. Chem.* **2009**, *48*, 5617. (l) Choi, S. W.; Ryu, D. W.; Lee, J. W.; Yoon, J. H.; Kim, H. C.; Lee, H.; Cho, B. K.; Hong, C. S. *Inorg. Chem.* **2009**, *48*, 9066. (m) Venkatakrishnan, T. S.; Sahoo, S.; Bréfuel, N.; Duhayon, C.; Paulsen, C.; Barra, A.-L.; Ramasesha, S.; Sutter, J.-P. *J. Am. Chem. Soc.* **2010**, *132*, 6047.

(8) (a) Bieksza, D. S.; Hendrickson, D. N. *Inorg. Chem.* **1977**, *16*, 924. (b) Beauvais, L. G.; Long, J. R. *J. Am. Chem. Soc.* **2002**, *124*, 2110. (c) Freedman, D. E.; Jenkins, D. M.; Long, J. R. *Chem. Commun.* **2009**, 4829.

(9) Marvaud, V.; Decroix, C.; Scuiller, A.; Guyard-Duhayon, C.; Vaissermann, J.; Gonnet, F.; Verdaguer, M. *Chem.−Eur. J.* **2003**, *9*, 1677.

(10) Harris, T. D.; Bennett, M. V.; Clérac, R.; Long, J. R. *J. Am. Chem. Soc.* **2010**, *132*, 3980.

(11) This equation applies in the infinite-size regime for an Ising-type single-chain magnet with the following definition of the Hamiltonian:

$$H = -2J\sum_{-\infty}^{+\infty}\vec{S}_i\vec{S}_{i+1} + D\sum_{-\infty}^{+\infty}\vec{S}_{iz}^2$$

and in the $|D/J| > 4/3$ Ising limit, where Δ_τ is the overall relaxation barrier, and S and D are the spin ground state and magnetic anisotropy parameter of the repeating unit, respectively. See: Coulon, C.; Clérac, R.; Lecren, L.; Wernsdorfer, W.; Miyasaka, H. *Phys. Rev. B* **2004**, *69*, 132408.

scopic detail for the first time through application of a modified Seiden model.

Experimental Section

Preparation of Compounds. General. The compound $(Bu_4N)_2[ReCl_4(CN)_2]\cdot 2DMA$ was prepared as previously reported.[10] All other reagents were obtained from commercial sources and used without further purification. **Caution!** Although we have experienced no problems while working with them, perchlorate salts are potentially explosive and should be handled with extreme care and only in small quantities.

$(Bu_4N)[TpCuReCl_4(CN)_2]\cdot 1.33CH_3CN$ (1). A solution of KTp (0.012 g, 0.049 mmol) in 6 mL of absolute ethanol was added dropwise to a vigorously stirred solution of $[Cu(ClO_4)_2]\cdot 6H_2O$ (0.024 g, 0.065 mmol) in 6 mL of absolute ethanol, resulting in a pale-blue solution and white precipitate. After stirring for 5 min, the white solid was removed via filtration through diatomaceous earth. The pale blue filtrate was then cooled to 0 °C in an ice water bath. A solution of $(Bu_4N)_2[ReCl_4(CN)_2]\cdot 2DMA$ (0.050 g, 0.048 mmol) in 6 mL acetonitrile was chilled to 0 °C and added dropwise to afford a pale green solution. After stirring for 10 min, the solution was filtered through diatomaceous earth to remove a small amount of insoluble green material, and the filtrate was quickly transferred to a 200 mL glass jar in a 3 °C refrigerator, while allowed to concentrate via evaporation. After 2 days, green blade-shaped crystals (21 mg, 46%) of product had formed. IR: $\bar{\nu}_{BH}$ 2521 cm^{-1}; $\bar{\nu}_{CN}$ 2289 (MeCN), 2246 (MeCN), 2165 (bridging) cm^{-1}. Due to the instability of crystals of **1** outside their mother liquor, acceptable elemental analysis has not been obtained. As such, all magnetic measurements (see below) were conducted on samples of crystals restrained in their frozen mother liquor.

X-ray analysis for **1** ($C_{29.66}H_{10}BCl_4CuN_{10.33}Re$, fw = 953.69 g/mol) at T = 175 K: space group $P2_1/c$, a = 11.4534(7), b = 16.2945(10), c = 22.1655(13) Å, β = 90.6770(10)°, V = 4136.4(4) Å^3, Z = 4, μ = 4.638 mm^{-1}, R_{int} = 0.0187, 60 769 reflections measured, 6336 independent reflections, R_1 = 0.0684, wR_2 = 0.1889.

X-Ray Structure Determinations. A single crystal of compound **1** was coated with Paratone-N oil and mounted on a Kaptan loop. The crystal was then quickly transferred to a Bruker Platinum 200 Instrument at the Advanced Light Source at the Lawrence Berkeley National Laboratory, and cooled in a stream of cold nitrogen. Preliminary cell data were collected to give a unit cell consistent with the tetragonal Laue group, and the unit cell parameters were later refined against all data. A full hemisphere of data was collected, and the crystal did not show significant decay during data collection. Data were integrated and corrected for Lorentz and polarization effects using SAINT v7.34 and were corrected for absorption effects using SADABS 2.10. Space group assignments were based upon systematic absences, E statistics, and successful refinement of the structures. The structure was solved by direct methods and expanded through successive difference Fourier maps. It was refined against all data using the SHELXTL 5.0 software package. Hydrogen atoms were placed in ideal positions and refined using a riding model. Thermal parameters for all non-hydrogen atoms pertaining to the chain were refined anisotropically. Due to crystal disorder, tetrabutylammonium cations and lattice acetonitrile molecules were refined isotropically.

Magnetic Susceptibility Measurements. Magnetic data were collected using a Quantum Design MPMS-XL SQUID magnetometer. Measurements for **1** were obtained for crystals (6.8 mg) covered and thus restrained in a minimum of their frozen mother liquor within a sealed straw to prevent desolvation of the solid. No evaporation of the mother liquor was observed during the measurements. A sample containing pure mother liquor was separately measured and found to exhibit a paramagnetic signal within error of the polycrystalline sample measurement. The mass of the sample was determined after the measurements and subsequent mother liquor evaporation. These measurements were collected in the temperature range 1.8−300 K and in the field range −7 to 7 T. An M vs H measurement was performed at 100 K to confirm the absence of ferromagnetic impurities. Ac magnetic susceptibility data were collected in zero dc field in the temperature range 1.8−10 K, under an ac field of 3 Oe, oscillating at frequencies in the range 1−1488 Hz. Ac susceptibility measurements show a complete absence of any out-of-phase component above 1.8 K at frequencies to 1500 Hz. The magnetic data were corrected for core diamagnetism of the sample.

Other Physical Measurements. Infrared spectra were obtained on a Perkin-Elmer Spectrum 100 Optica FTIR spectrometer, equipped with an attenuated total reflectance accessory (ATR).

Results and Discussion

Synthesis and Structural Analysis. The compound $(Bu_4N)[TpCuReCl_4(CN)_2]\cdot 1.33CH_3CN$ (**1**) was synthesized through addition of $[ReCl_4(CN)_2]^{2-}$ to a solution containing $[Cu(MeCN)_6]^{2+}$ and KTp in a mixture of ethanol and acetonitrile at 0 °C, followed by crystallization at 3 °C to afford green plate-shaped crystals suitable for X-ray diffraction. The structure of **1**, depicted in Figure 1, consists of one-dimensional zigzag chains that propagate along the b axis, where each chain is composed of alternating $[ReCl_4(CN)_2]^{2-}$ and $[TpCu]^+$ units, bridged through cyanide. To our knowledge, **1** represents the first structurally characterized example of a cyanide bridge between rhenium and copper not supported by a $Re_{6-n}Os_nQ_8$ (n = 0, 1, 2; Q = chalcogenide)[12] or Re_4Q_4[13] cluster core. The coordination environment of each Re^{IV} center does not deviate significantly from that in $[ReCl_4(CN)_2]^{2-}$, and each Cu^{II} center approximates a square pyramidal coordination geometry (see Table S1, Figures S1 and S2, Supporting Information). Each Cu^{II} center exhibits a significant Jahn−Teller elongation along the $Cu-N_{apical}$ bond and subsequent contraction along the $Cu-N_{basal}$ and CuN_{CN} bonds, giving rise to bond distances of $d_{Cu-N(apical)}$ = 2.1828(1) Å, $d_{Cu-N(CN)}$ = 2.0130(1) Å (mean), and $d_{Cu-N(basal)}$ = 1.9839(1) Å (mean). The mean Re−C−N angles do not deviate significantly from linearity, while the Cu−N−C angles are slightly more bent, with a mean angle of 168.96(1)°. Note, however, that the Cu−N−C angles are considerably less bent than those found in the $(DMF)_4MReCl_4(CN)_2$ (M = Mn, Fe, Co, Ni) chain compounds, where the mean M−N-C angle is 158.l(1)°. This substantial increase enhances the orthogonality of the $d_{\pi(Re)}$ and $d_{\sigma(Cu)}$ orbitals and should thus promote stronger ferromagnetic exchange. Along the c axis, neighboring chains are linked through $\pi-\pi$ stacking of pyrazolate rings, with a ring centroid separation of 3.4985(2) Å (see Figure 1, middle), resulting in the formation of two-dimensional sheets of chains lying in the bc plane. Each pair of stacked pyrazolate rings are coplanar, with a slip angle between the ring plane and centroid-centroid vector of 78.052(4)°. Along the a axis, these sheets are well separated from one another by tetrabutylammonium cations and lattice acetonitrile molecules (see Figure 1, lower), with a shortest intersheet metal−metal distance of d_{Cu-Cu} = 11.4534(7) Å.

(12) (a) Tulsky, E. G.; Crawford, N. R. M.; Baudron, S. A.; Batail, P.; Long, J. R. *J. Am. Chem. Soc.* **2003**, *125*, 15543. (b) Mironov, Y. V.; Naumov, N. G.; Brylev, K. A.; Efremova, O. A.; Fedorov, V. E.; Hegetschweiler, K. *Angew. Chem.* **2004**, *116*, 1317. *Angew. Chem., Int. Ed.* **2004**, *43*, 1297. (c) Mironov, Y. V.; Naumov, N. G.; Brylev, K. A.; Efremova, O. A.; Fedorov, V. E.; Hegetschweiler, K. *Koord. Khim.* **2005**, *31*, 289. (d) Brylev, K. A.; Pilet, G.; Naumov, N. G.; Perrin, A.; Fedorov, V. E. *Eur. J. Inorg. Chem.* **2005**, 461. (e) Naumov, N. G.; Mironov, Y. V.; Brylev, K. A.; Fedorov, V. E. *Zh. Strukt. Khim.* **2006**, *47*, 782. (f) Xu, L.; Kim, Y.; Kim, S.-J.; Kim, H. J.; Kim, C. *Inorg. Chem. Commun.* **2007**, *10*, 586.

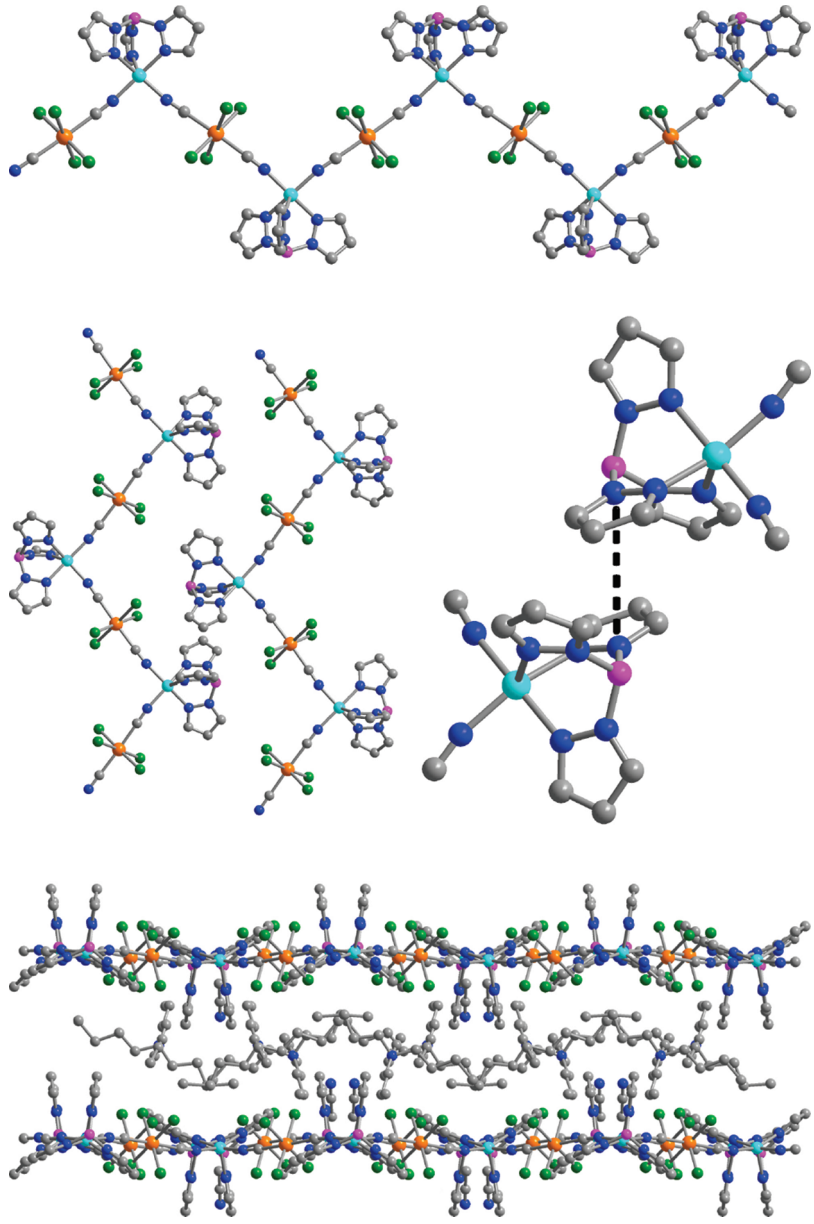

Figure 1. Upper: Crystal structure of $(Bu_4N)[TpCuReCl_4(CN)_2]$, as observed in **1**. Orange, cyan, green, purple, gray, and blue spheres represent Re, Cu, Cl, B, C, and N atoms, respectively; H atoms are omitted for clarity. Middle Left: View along the *a* axis, illustrating the arrangement of neighboring chains to form a two-dimensional sheet. Middle Right: View of $\pi-\pi$ stacking between pyrazolate rings of neighboring chains, where $d = 3.4985(2)$ Å. Lower: View along the *c* axis, where the sheets of chains are separated by Bu_4N^+ cations, with a shortest intersheet metal−metal distance of 11.4534(7) Å.

Static Magnetic Properties Above 12 K. To probe the magnetic exchange coupling in **1**, variable-temperature magnetic susceptibility data were collected. A plot of $\chi_M T$ vs T, recorded in an applied dc field of 1000 Oe, is shown in Figure 2. At 300 K, $\chi_M T = 2.0$ cm^3 K/mol, which is slightly higher than the value expected for one isolated Re^{IV} center ($S = {}^3/_2$, $g \approx 1.65$)[10] and one isolated Cu^{II} center ($S = {}^1/_2$, $g \approx 2.0$). Upon lowering the temperature from 300 K, $\chi_M T$ begins a gradual increase, then climbs abruptly below 80 K to reach a maximum of 9.6 cm^3 K/mol at 12 K. This behavior is indicative of intrachain ferromagnetic coupling between the Re^{IV} ($t_{2g}{}^3$) and Cu^{II} ($e^4b_2{}^2b_1{}^2a_1{}^1$) centers, as expected for superexchange through cyanide.[14] In order to quantify the strength of intrachain exchange coupling, $J_{||}$, in **1**, the $\chi_M T$ data were modeled considering a Heisenberg chain comprised of alternating isotropic classical ($S_i = {}^3/_2$ for Re^{IV} site) and quantum ($s_i = {}^1/_2$ for Cu^{II} metal ions) spins, and thus the following spin Hamiltonian was used in the analysis:

$$H_{||} = -2J_{||}\sum_{i=1}^{N}((\vec{s}_i + \vec{s}_{i+1}) \bullet \vec{S}_i)$$

At a first glance, use of an isotropic Heisenberg model to describe the high temperature magnetic properties of **1** may seem inappropriate, considering the presence of the highly anisotropic $[ReCl_4(CN)_2]^{2-}$ unit inside the chain.[10] As such, in order to determine the temperature domain in which the anisotropy can be neglected, the correlation length, ξ, of the system was analyzed. Experimentally, ξ can be readily estimated, as it is directly proportional to the $\chi_M T$ product.[15,16] In the isotropic Heisenberg case, ξ is expected to increase linearly with inverse temperature.[17] As shown in Figure 3, the linear growth of the correlation length is experimentally confirmed above 12 K, thus demonstrating the efficacy of an isotropic Heisenberg model above this temperature. The data were fit in the temperature range 12−300 K, employing a Seiden expression previously

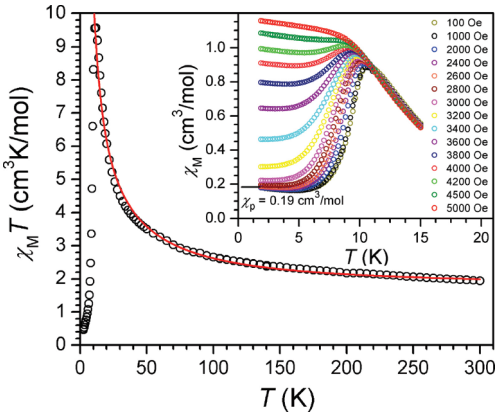

Figure 2. Variable-temperature magnetic susceptibility data for **1** (where χ_M is the molar magnetic susceptibility obtained as $\chi_M = M/H$), collected under a dc field of 1000 Oe. The solid red line corresponds to a fit to the data, as described in the text. Inset: Variable-temperature magnetic susceptibility data, collected under various applied dc fields.

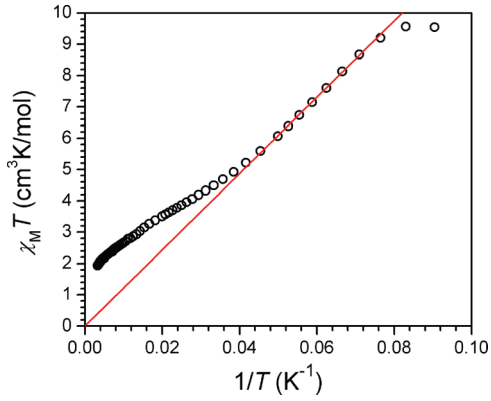

Figure 3. Plot of $\chi_M T$ vs $1/T$ data for **1** (where χ_M is the molar magnetic susceptibility obtained as $\chi_M = M/H$), collected under a dc field of 1000 Oe. The solid red line corresponds to the linear regime observed between 30 and 12 K.

used to describe the magnetic susceptibility of an alternating chain,[18] to give $J_{||}/k_B = +41(2)$ K ($+29$ cm^{-1}) and $g_{av} = 1.74(1)$. To our knowledge, this value of $J_{||}$ represents the strongest ferromagnetic superexchange interaction yet reported through cyanide, eclipsing the mark of $J = +23$ cm^{-1} measured for the heptanuclear cluster $[(tren)_6Cu_6Cr(CN)_6]^{9+}$ (tren = tris(2-amino)ethylamine).[3d] Such strong magnetic coupling arises from

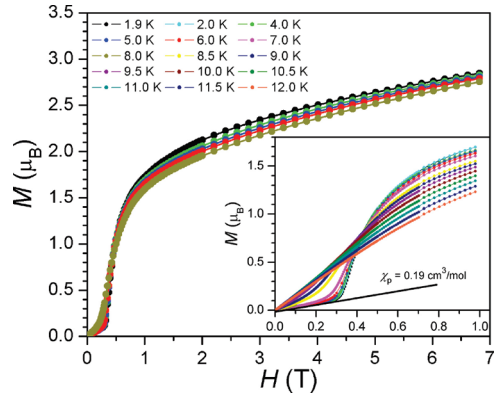

Figure 4. Variable-field magnetization data for **1**, collected at various temperatures. Inset: Expanded view of the data, highlighting inflection point that shifts to lower field with increasing temperature.

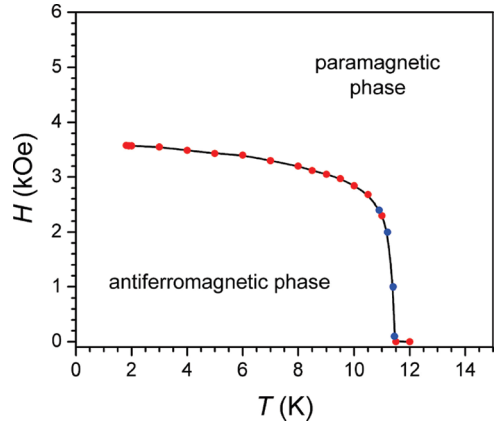

Figure 5. Magnetic (T, H) phase diagram for **1**, constructed from variable-field (blue circles) and variable-temperature (red circles) magnetic susceptibility data. The solid black line is a guide for the eye.

the presence of a d^9 electron configuration with local C_{4v} symmetry. The square pyramidal coordination of the Cu^{II} center serves to lower the energy of the d_{z^2} orbital relative to the $d_{x^2-y^2}$ orbital, thereby localizing the unpaired electron along the $Cu-N_{CN}$ bond, in the direction of magnetic exchange.

Extracting and Modeling the Magnetic Phase Diagram. Below 12 K at 1000 Oe, $\chi_M T$ undergoes a precipitous decline, reaching a minimum of 0.5 cm^3 K/mol at 1.8 K (see Figure 2). To probe this downturn, variable-temperature susceptibility measurements were conducted under various applied dc fields (see Figure 2, inset). The maximum of the magnetic susceptibility shifts to lower temperature with increasing applied field, until the data reach a plateau at $H \geq 4500$ Oe. The strong field dependence of the susceptibility suggests the presence of a magnetic phase transition below 12 K. To further investigate that possibility, variable-field magnetization data were collected at multiple temperatures between 1.9 and 12 K (see Figure 4). Indeed, the magnetization curve exhibits a temperature-dependent inflection point, corresponding to a maximum in the field dependence of the susceptibility, $\chi_M = dM/dH$ (see Figure S3, Supporting Information), that is associated with a characteristic field, H_C. By combining the maxima observed in the $\chi_M(T)$ and $\chi_M(H)$ data, a (T,H) phase diagram can be constructed (see Figure 5), providing a complete map of the temperature dependence of H_C. Note that the phase transition curve extrapolates to $T = 0$ K at approximately $H_C(0) = 3600$ Oe and vanishes near $T_N = 11.4$ K. The phase diagram is typical

(13) (a) Mironov, Y. V.; Fedorov, V. E.; Ijjaali, I.; Ibers, J. A. *Inorg. Chem.* **2001**, *40*, 6320. (b) Mironov, Y. V.; Efremova, O. A.; Naumov, D. Y.; Sheldrick, W. S.; Fedorov, V. E. *Eur. J. Inorg. Chem.* **2003**, 2591. (c) Mironov, Y. V.; Efremova, O. A.; Solodovnikov, S. F.; Naumov, N. G.; Sheldrick, W. S.; Perrin, A.; Fedorov, V. E. *Izv. Akad. Nauk SSSR, Ser. Khim.* **2004**, 2040. (d) Efremova, O. A.; Mironov, Y. V.; Naumov, D. Y.; Kozlova, S. G.; Fedorov, V. E. *Polyhedron* **2006**, *25*, 1233. (e) Efremova, O. A.; Mironov, Y. V.; Naumov, D. Y.; Fedorov, V. E. *Zh. Strukt. Khim.* **2006**, *47*, 754.
(14) (a) Entley, W. R.; Trentway, C. R.; Girolami, G. S. *Mol. Cryst. Liq. Cryst.* **1995**, *273*, 153. (b) Weihe, H.; Güdel, H. U. *Comments Inorg. Chem.* **2000**, *22*, 75.
(15) Coulon, C.; Miyasaka, H.; Clérac, R. *Struct. Bonding (Berlin)* **2006**, *122*, 163.
(16) See for example: Thompson, C. J. *Phase transitions and critical phenomena*; Domb, C., Green, M. S., Eds.; Academic Press: London, NY, 1972; Vol. 1, p 177.
(17) (a) Fisher, M. E. *Am. J. Phys.* **1964**, *32*, 343. (b) Yamada, M. *J. Phys. Soc. Jpn.* **1990**, *59*, 848.
(18) Seiden, J. *J. Phys., Lett.* **1983**, *44*, L947. Note that the intrachain exchange is written $2J_{||}$ in this work, while it is equal to the coupling constant J introduced by Seiden.

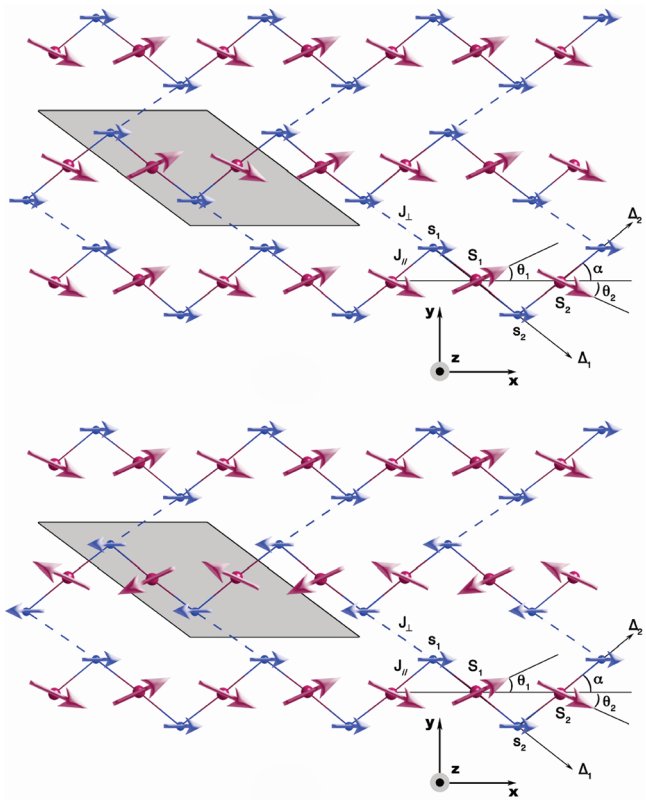

Figure 6. Schematic representation of the $T = 0$ K magnetic superstructure in the antiferromagnetic (i.e., zero-magnetic field; bottom) and paramagnetic (i.e., above the critical field in the $\boldsymbol{x}$ direction; top) phases in the *bc* plane; the blue and purple spheres/arrows represent Cu^{II} and Re^{IV} ions, respectively; the colored solid lines between the atoms represent the cyanide bridges, and the dashed lines represent the interchain coupling through the pyrazolate rings interactions. The gray parallelepiped represents the 1D magnetic unit cell.

of an antiferromagnet with a metamagnetic behavior, such that the $H_C(T)$ line corresponds to an antiferromagnetic/paramagnetic phase transition that occurs when the magnetic field is applied along the easy direction of the magnetization (defined as the x magnetic axis along the chains). The occurrence of long-range magnetic order likely stems from the presence of transverse $\pi-\pi$ interactions, with magnitude $J_\perp$, between Cu^{II} centers through the pyrazolate rings on neighboring chains (see Figures 1 and 6). Indeed, previous reports have described similar metamagnetic behavior in one-dimensional chain compounds arising from $\pi-\pi$ stacking of aromatic rings on adjacent chains.[19] As such, $J_\perp$ can be modeled according to the following interchain Hamiltonian using the notations of Figure 6, where i and j are indexes for the spin i in the chain j:

$$H_\perp = -2J_\perp \sum_{i,j} \vec{s}_{1,i,j}\vec{s}_{1,i,j+1} - 2J_\perp \sum_{i,j} \vec{s}_{2,i,j}\vec{s}_{2,i,j-1}$$

At $T = 0$ K, the magnetic field necessary to align the chain magnetization of the two antiferromagnetic sublattices, and thereby overcome the ordering, is $H_C(0) = 3600$ Oe. Thus, by equating the Zeeman and transverse (interchain) exchange energies, $2|J_\perp|s^2 = (g_S S + g_s s)\mu_B H_C(0)$, the value of the interchain exchange parameter can be obtained. Indeed, this treatment reveals a value of $J_\perp/k_B = -1.7$ K (-1.2 cm^{-1}), with $g_s = 2.0$ and $g_S = 1.65$.[10]

In a quasi-one-dimensional description, the mean field interchain Hamiltonian, H_{mf}, can be used to determine the transition temperature in zero dc field.[20] Introducing the effective field, $\vec{H}_{eff}$ seen by the isotropic $\vec{s}$ spins, the expression of H_{mf} deduced from $H_\perp$ is given by:[21]

$$H_{mf} = -4J_\perp\langle\vec{s}\rangle\sum_{i,j}\vec{s}_{i,j} = -\vec{H}_{eff}\sum_{i,j}\vec{\mu}_{s_{i,j}}$$

where

$$\vec{H}_{eff} = \frac{4J_\perp}{(g_s\mu_B)^2}\langle\vec{\mu}_s\rangle$$

As the experimental data demonstrate the presence of an antiferromagnetic ground state (see Figure 5), the second-order phase transition toward the ordered magnetic phase is determined from the divergence of the staggered magnetic susceptibility. This problem can be simplified by changing the sign of the interchain exchange to positive and searching for the divergence of the static magnetic susceptibility. Following a Seiden model (see eq 26 in ref 18), this susceptibility in the one-dimensional case is:

$$\chi_M = \frac{1}{k_B T}\sum_{i,j}\langle(\mu^z_{S_i} + \mu^z_{s_i})(\mu^z_{S_j} + \mu^z_{s_j})\rangle$$

for which the thermodynamic average is taken in zero applied field. As $\vec{S}$ are classical spins such that $\vec{S}$ and $\vec{s}$ commute, this expression can be readily separated into two parts to deduce separately the thermodynamic average of the magnetic moment for each kind of spin, as follows:

$$\langle\mu^z_S\rangle = \frac{1}{k_B T}\sum_{i,j}\langle\mu^z_{S_i}(\mu^z_{S_j}H + \mu^z_{s_j}H)\rangle$$

and

$$\langle\mu^z_s\rangle = \frac{1}{k_B T}\sum_{i,j}\langle\mu^z_{s_i}(\mu^z_{S_j}H + \mu^z_{s_j}H)\rangle$$

These two equations can then be transposed in the quasi-one-dimensional case at the mean field approximation, introducing H_{eff}:

$$\langle\mu^z_S\rangle = \frac{1}{k_B T}\sum_{i,j}\langle\mu^z_{S_i}(\mu^z_{S_j}H + \mu^z_{s_j}(H + H_{eff}))\rangle$$

and

$$\langle\mu^z_s\rangle = \frac{1}{k_B T}\sum_{i,j}\langle\mu^z_{s_i}(\mu^z_{S_j}H + \mu^z_{s_j}(H + H_{eff}))\rangle$$

Introducing the correlation functions calculated by Seiden,[18] $S_{\alpha\gamma} = \sum_{i,j}\langle\mu^z_{\alpha_i}\mu^z_{\gamma_j}\rangle$ (with the $\alpha\gamma$ index stands for *ss*, *Ss* or *SS*)

(19) (a) Yoon, J. H.; Kim, H. C.; Hong, C. S. *Inorg. Chem.* **2005**, *44*, 7714. (b) Wen, H.-R.; Wang, C.-F.; Song, Y.; Gao, S.; Zuo, J.-L.; You, X.-Z. *Inorg. Chem.* **2006**, *45*, 8942. (c) Yoon, J. H.; Lim, J. H.; Choi, S. W.; Kim, H. C.; Hong, C. S. *Inorg. Chem.* **2007**, *46*, 1529. (d) Wang, S.; Ferbinteanu, M.; Yamashita, M. *Inorg. Chem.* **2007**, *46*, 610. (e) Choi, S. W.; Kwak, H. Y.; Yoon, J. H.; Kim, H. C.; Koh, E. K.; Hong, C. S. *Inorg. Chem.* **2008**, *47*, 10214.

(20) See Part 1 of the following reference: Scalapino, D. J.; Imry, Y.; Pincus, P. *Phys. Rev. B* **1975**, *11*, 2042.

(21) See Part 1 of the theoretical Supporting Information on the magnetic analysis.

and $\lambda = 4|J_\perp|/(g_s\mu_B)^2$, the average magnetic moment of each spin can be expressed as follows:

$$\langle\mu_S^z\rangle = \frac{1}{k_B T}(S_{SS}H + S_{Ss}H + \lambda S_{Ss}\langle\mu_s^z\rangle)$$

and

$$\langle\mu_s^z\rangle = \frac{1}{k_B T}(S_{Ss}H + S_{ss}H + \lambda S_{ss}\langle\mu_s^z\rangle)$$

or after simplifications,

$$\langle\mu_s^z\rangle = \frac{(S_{Ss} + S_{ss})}{k_B T - \lambda S_{ss}}H$$

and

$$\langle\mu_S^z\rangle = \frac{(S_{SS} + S_{Ss})}{k_B T}H + \frac{1}{k_B T}\frac{\lambda S_{Ss}(S_{Ss} + S_{ss})H}{k_B T - \lambda S_{ss}}$$

From these expressions, the magnetic susceptibility is easily obtained as follows:

$$\chi_M = \frac{\langle\mu_S^z\rangle + \langle\mu_s^z\rangle}{H} = \frac{(S_{SS} + S_{Ss})}{k_B T} + \frac{\left(1 + \frac{\lambda S_{Ss}}{k_B T}\right)(S_{Ss} + S_{ss})}{k_B T - \lambda S_{ss}}$$

The transition temperature can then be deduced from the divergence of χ_M (i.e., $k_B T_C - \lambda S_{ss} = 0$, either with ferromagnetic or antiferromagnetic interchain couplings), according to the following expression:

$$\frac{4|J_\perp|}{(g_s\mu_B)^2}S_{ss}(T_C) = k_B T_C$$

To give an explicit expression of the transition temperature, the expression of S_{ss} given by Seiden (see eq 27 in ref 18) should be used in the low temperature limit (see eq 24 in ref 18). Finally, the transition temperature can be calculated as follows:

$$k_B T_N = \sqrt{|J_\perp|J_{||}S}$$

We note that this expression is general for any one-dimensional system with an alternation of classical (S) and quantum $s = 1/2$ isotropic spins with interchain interactions localized between quantum spins. Insertion of $J_\perp/k_B = -1.7$ K (-1.2 cm^{-1}) and $J_{||}/k_B = +41$ K ($+29$ cm^{-1}) into this last equation provides a critical temperature of $T_N = 10.2$ K, in good agreement with the experimental value of 11.4 K. Nevertheless, the observed small discrepancy on T_N might arise from the intrinsic Ising-like anisotropy of the $[ReCl_4(CN)_2]^{2-}$ unit, which magnetization measurements indicate possesses an axial zero-field splitting parameter of $D/k_B = -20.1$ K (-14.4 cm^{-1}) as a tetrabutylammonium salt.[10]

Determination of the Local Magnetic Anisotropy. To estimate the anisotropy strength for each $[ReCl_4(CN)_2]^{2-}$ unit along the zigzag chain, the theoretical powder susceptibility at 0 K and in the weak field approximation has to be calculated and compared to the experimental data ($\chi_p = 0.19$ cm^3/mol) below 2000 Oe and at 1.8 K on the χ_M vs T or M vs H plots (see Figures 2 and 4). On a powder sample, the measured susceptibility is given as follows:

$$\chi_p = \frac{1}{3}(\chi_{xx} + \chi_{yy} + \chi_{zz})$$

To estimate the three components of the magnetic susceptibility, the magnetic superstructures shown in the Figure 6 must first be addressed. Figure 6 depicts the equilibrium position of the spins in the absence of an applied magnetic field (see bottom panel) or when a field is applied along the x direction slightly above the transition field (see top panel). In this direction, the magnetic field induces a sudden rotation of the magnetic moment at H_C. In contrast, applying the magnetic field along y or z implies a continuous rotation of the magnetic moments. The consequence at low temperature is a vanishing initial magnetic susceptibility along x when the applied magnetic field is small, while the initial susceptibility remains finite down to $T = 0$ K when the magnetic field is applied along y or z. In the CuRe chain, the y and z components of the susceptibility are given by the following expressions (see the Supporting Information for a complete description of the calculations):[22]

$$\chi_{yy} \approx \frac{(\mu_S + \mu_s)^2}{A_1|D|S^2 + 2|J_\perp|}$$

and

$$\chi_{zz} \approx \frac{(\mu_S + \mu_s)^2}{A_2^2|D|S^2 + 2|J_\perp|}$$

with

$$A_1 = \cos 2\alpha + \frac{|D|S^2 \sin^2 2\alpha}{2J_{||}Ss + |D|S^2 \cos 2\alpha}$$

and

$$A_2 = \cos \alpha + \frac{|D|S^2 \sin \alpha \sin 2\alpha}{4J_{||}Ss + 2|D|S^2 \cos 2\alpha}$$

As expected, the transverse susceptibilities are proportional to the inverse of the sum of anisotropy and transverse exchange terms. As the susceptibility along x is zero at low fields, the powder susceptibility is thus given as follows:

$$\chi_p \approx \frac{(\mu_S + \mu_s)^2}{3}\left(\frac{1}{A_1|D|S^2 + 2|J_\perp|} + \frac{1}{A_2^2|D|S^2 + 2|J_\perp|}\right)$$

Considering the two exchange constants, $J_{||}/k_B = +41$ K and $J_\perp/k_B = -1.7$ K, along with the zigzag angle of the chain, $\alpha = 38.7°$ (as defined in Figure 6) and $\chi_p = 0.19$ cm^3/mol, the local anisotropy energy of each $S = {}^3/_2$ $[ReCl_4(CN)_2]^{2-}$ unit is estimated to be $DS^2/k_B \approx -20$ K (-14 cm^{-1}) or $D/k_B \approx -9$ K (-6 cm^{-1}). The presence of this anisotropy explains the observed difference between the theoretical Heisenberg and experimental values of T_N. Importantly, while this value of D is quite large, the effective anisotropy of the chain is much smaller due to its canting topology and an α angle close to 45°.[22] The weak effective anisotropy likely explains the absence of

(22) See Part 2 of the theoretical Supporting Information on the magnetic analysis.

single-chain magnet behavior, or related magnet-like properties within an ordered antiferromagnetic phase of single-chain magnets.[23]

Conclusions and Outlook

The foregoing results demonstrate the use of $[ReCl_4(CN)_2]^{2-}$ in the synthesis of a one-dimensional zigzag chain compound of formula $(Bu_4N)[TpCuReCl_4(CN)_2]$. Within the solid, individual chains display ferromagnetic coupling between Re^{IV} and Cu^{II} centers of unprecedented strength through the cyanide bridge, thus demonstrating the utility of the $Re^{IV}-CN-Cu^{II}$ linkage in constructing strongly coupled magnetic materials. In addition, a Seiden model has been applied to describe the critical magnetic behavior of the compound. Finally, we demonstrate experimentally and theoretically that the zigzag arrangement of the local tensors of magnetic anisotropy around the Re^{IV} ions dramatically reduces the effective magnetic anisotropy of the chain, thus explaining the absence of slow relaxation despite the strong one-dimensional exchange. Work is underway to construct other one-dimensional solids based on the $Re^{IV}-CN-Cu^{II}$ linkage that feature a linear arrangement of the metal centers within the chains, such that the local anisotropy tensors do not cancel. In addition, future work will target related compounds with greater interchain separations to preclude magnetic ordering at low temperature. It is our expectation that these synthetic efforts will enable utilization of strong ferromagnetic coupling in the assembly of new single-chain magnets with large relaxation energy barriers.

Acknowledgment. This work was supported by NSF grant No. CHE-0617063, the France-Berkeley Fund, the University of Bordeaux, ANR (NT09_469563, AC-MAGnets project), Région Aquitaine, GIS Advanced Materials in Aquitaine (COMET Project), MAGMANet (NMP3-CT-2005-515767) and CNRS. We thank Tyco Electronics for fellowship support of T.D.H. and Dr. D. Freedman for experimental assistance.

Supporting Information Available: Crystallographic files (CIF) and plots showing additional data. This material is available free of charge via the Internet at http://pubs.acs.org.

JA108575T

(23) (a) Coulon, C.; Clérac, R.; Wernsdorfer, W.; Colin, T.; Miyasaka, H. *Phys. Rev. Lett.* **2009**, *102*, 167204/1–4. (b) Miyasaka, H.; Takayama, K.; Saitoh, A.; Furukawa, S.; Yamashita, M.; Clérac, R. *Chem.—Eur. J.* **2010**, 3656.